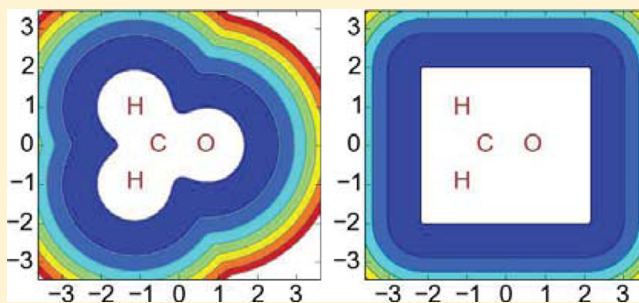


# Complex Absorbing Potentials with Voronoi Isosurfaces Wrapping Perfectly around Molecules

Thomas Sommerfeld<sup>\*,†</sup> and Masahiro Ehara<sup>\*,‡</sup><sup>†</sup>Department of Chemistry and Physics, Southeastern Louisiana University, SLU 10878, Hammond, Louisiana 70402, United States<sup>‡</sup>Institute for Molecular Science, Research Center for Computational Science, Myodai-ji, Okazaki 444-8585, Japan

## S Supporting Information

**ABSTRACT:** Complex absorbing potentials (CAPs) are imaginary potentials that are added to a Hamiltonian to change the boundary conditions of the problem from scattering to square-integrable. In other words, with a CAP, standard bound-state methods can be used in problems involving unbound states such as identifying resonance states and predicting their energies and lifetimes. Although in wave packet dynamics, many CAP forms are used, in electronic structure theory, the so-called box-CAP is used almost exclusively, because of the ease of evaluating its integrals in a Gaussian basis set. However, the box-CAP does have certain disadvantages. First, it will, e.g., break the symmetry of  $C_{nv}$  molecules if  $n$  is odd and the main axis is placed along the  $z$ -axis by the “standard orientation” of the electronic structure code. Second, it provides a CAP starting at the smallest box around the entire molecular system. For larger molecules or clusters, which do not fill the space efficiently, that implies that much “dead space” within the molecule will be left, where there is neither a CAP nor a sufficient description with basis functions. Here, two new CAP forms are introduced and systematically explored: first, a Voronoi-CAP (that is, a CAP defined in each atom’s Voronoi cell), and second, a smooth Voronoi-CAP (which is similar to the Voronoi-CAP; however, the noncontinuously differentiable behavior at the surfaces between the Voronoi cells is smoothed out). Both have isosurfaces that are similar to the cavities used in solvation modeling. An obvious disadvantage of these two CAPs is that the integrals cannot be obtained analytically, but must be computed numerically. However, Voronoi-CAPs share the advantage of having the same symmetry as the molecular system, and, more importantly, considerably facilitate the treatment of larger molecules with asymmetric side chains and of molecular clusters.



## 1. INTRODUCTION

Complex absorbing potentials (CAPs) have been successfully applied in many contexts, from nuclear physics, over vibrational predissociation and reactive scattering phenomena, to electronically metastable states.<sup>1,2</sup> In the context of electronic structure, CAPs are used to characterize resonances, such as temporary anions and dianions, core ionized states (Auger decay), and molecules subjected to field ionization.<sup>3–10</sup> Here, the focus is the choice of the CAP itself, and temporary anions will be used as examples.

In the CAP method, a negative imaginary potential,  $-i\eta W$ , which is intended to absorb the emitted excess electron, is added to the Hamiltonian of the system, where  $\eta$  refers to the CAP strength, and  $W$  is a normally real, positive potential, which grows as one moves away from the system.<sup>1,11</sup> Provided the CAP is sufficiently strong to absorb the electron within the limitations of the basis set (limitations can be both in position and in momentum space), the resonance is described by a single state with a square-integrable wave function and a complex eigenvalue  $E_{\text{res}} = E_r - i\Gamma/2$  with the real part,  $E_r$ , being the resonance energy or resonance position and the imaginary part,  $\Gamma/2$ , being the half width, which is directly related to the lifetime  $\tau$  of the metastable state ( $\tau = \hbar/\Gamma$ ).

An ideal CAP needs to fulfill three conflicting requirements: First, it should perturb the original system as little as possible, that is, it should be negligible at the system. Second, at its onset, it should grow smoothly and slowly so as not to cause any artificial reflections of the outgoing electron. And third, the CAP must be strong enough to absorb the electron within the confinement of the basis set, because otherwise the electron will be reflected at the “edge” of the basis set, again, causing artifacts. In other words, CAP calculations always involve compromises regarding CAP placement, shape, and strength, to minimize artificial reflections caused by the CAP itself and the basis set edge.

While it is fairly straightforward to optimize a CAP/basis set combination in the context of grid basis sets, this task is far more challenging in the context of Gaussian basis sets. Early applications for diatomic molecules employed simple functional forms for  $W$ , such as quadratic and cubic potentials about the center of mass, but the workhorse potential used in most CAP calculations today is a soft-box potential, the so-called “box-CAP”.<sup>12</sup>

Received: May 20, 2015



$$W^{(B)}(\vec{r}; \vec{c}) = W_x^{(B)}(r_x; c_x) + W_y^{(B)}(r_y; c_y) + W_z^{(B)}(r_z; c_z) \quad (1)$$

For electrons, this consists of three Cartesian components:

$$W_i^{(B)}(r_i; c_i) = \begin{cases} (r_i + c_i)^2 & r_i < -c_i \\ 0 & -c_i \leq r_i \leq c_i \\ (r_i - c_i)^2 & c_i < r_i \end{cases} \quad (2)$$

Here,  $\vec{r}$  is the position of the electron and  $\vec{c}$  is a vector of three cutoff parameters that determine the shape of the box.

In a Gaussian basis set, the box-CAP has the overwhelming advantage that the associated integrals can be evaluated analytically. However, the price one must pay is the rigid box-like shape, which fits most small, high-symmetry molecules well, but will clearly be less suitable for less-symmetrical molecules (e.g., molecules with asymmetric side chains or molecular clusters). Even for some small molecules, the box-CAP has a practical disadvantage whenever the quantum chemistry code employed centers the molecule in a “standard orientation”, since the box orientation is, for example, incompatible with the  $C_3$ -axis of a  $C_{3v}$  symmetrical molecule in the  $z$ -axis.

Here, two different approaches are explored: first, a Voronoi-CAP (that is, a CAP that is defined in each atom's Voronoi cell), and second, a smooth Voronoi-CAP (which is similar to the Voronoi-CAP, except that the sharp edges between the Voronoi cells are smoothed out). The first of these two potentials has an angular behavior that is similar to that of a CAP used recently in the investigation of strong-field laser ionization,<sup>8,13</sup> but the radial shape is different. An obvious disadvantage is that the integrals of the Voronoi-CAPs cannot be obtained analytically, but must be computed via numerical quadrature schemes. However, Voronoi-CAPs wrap perfectly around any molecule, and have, by definition, the same symmetry as the molecule. In addition, the number of cutoff parameters in the CAP is reduced from three to one, which makes it easier to explore the parameter space and “optimize” a CAP at a new geometry—if that is desired.

In the following, after a brief review of practical aspects of CAP calculations aimed at establishing some terminology and notation, the Voronoi-CAPs and their integral evaluation is described. Results obtained with the two Voronoi-CAPs then are compared with the box-CAP, using, as prototypical examples, the  $^2\Pi_g$  resonance of  $N_2$ , the  $^2B_1$  resonance of  $CH_2O$ , and the  $^2\Pi_u$  resonance of  $CO_2$ . Last, the new smooth Voronoi-CAP is applied to a model  $N_2(H_2O)_2$  cluster.

## 2. METHODS

**2.1. Absorbing Potentials.** In the CAP method, an absorbing potential,  $-i\eta W$ , is added to the molecular Hamiltonian  $H$ , generating a parametrized complex Hamiltonian:

$$H(\eta) = H - i\eta W \quad (3)$$

Here,  $W$  is a normally real potential that should ideally vanish at the molecular system and smoothly increase as the distance from the molecule increases, and  $\eta$  is a strength parameter. Resonances can then be distinguished from continuum solutions by computing the eigenvalues of  $H(\eta)$ . With a grain of salt, the continuum states will be “rotated” on a spectral string, whose particular shape is dependent on the particular

form of  $W$ , whereas resonances will appear as isolated poles at their complex energies  $E_r - i\Gamma/2$ .<sup>1,11</sup> With a complete basis set, the true resonance energy is obtained in the limit  $\eta \rightarrow 0$ . With a finite basis set, the CAP must be sufficiently strong to absorb the outgoing electron within the confinement of the basis set, and a compromise between a CAP that is too weak, which causes artificial reflections of the outgoing electron at the edge of the basis set, and a CAP that is too strong, which causes artificial reflections all by itself, must be found. To do so, one studies the so-called  $\eta$  trajectories of the eigenvalues of  $H(\eta)$  computed in a finite basis set. Provided the basis set is not too inflexible, pseudo-continuum states will accelerate comparatively quickly into the complex energy plane when  $\eta$  is increased, whereas eigenvalues associated with resonances will move more slowly and should show a stabilization behavior: The  $\eta$  trajectory should slow significantly, before accelerating again. It is this point of lowest “speed” that defines the best approximation for the resonance given a particular basis set.<sup>11</sup> Again, the less flexible the basis set, the less pronounced the stabilization of the resonance trajectories with consequences for precision and the ability to make predictions. To address low basis set quality, a series of corrections can be computed; yet, experience shows that going beyond first order is normally not necessary if reasonably large basis sets are used.<sup>1,14,15</sup> We will report both uncorrected and corrected values for two examples, but then restrict ourselves to corrected ones.

As mentioned above, in most CAP calculations reported so far, the potential  $W$  is the box-CAP  $W^{(B)}$  (see eq 1).<sup>12</sup> Here, we investigate the performance of two new CAPs that, similar to a van der Waals surface, wrap perfectly around the molecule. The first is the Voronoi-CAP, where the distance to the molecular system is defined through the distance to the nearest atom:

$$r_{\text{nearest}}(\vec{r}) = \min_{\alpha} (|\vec{r} - \vec{R}_{\alpha}|) \quad (4)$$

where the  $\vec{R}_{\alpha}$  are the positions of the nuclei. The Voronoi-CAP itself is then defined as

$$W^{(V)}(\vec{r}) = W^{(V)}(r_{\text{nearest}}) = \begin{cases} 0 & r_{\text{nearest}} \leq r_{\text{cut}} \\ (r_{\text{nearest}} - r_{\text{cut}})^2 & r_{\text{nearest}} > r_{\text{cut}} \end{cases} \quad (5)$$

and an example is shown in Figure 1. A similar potential—albeit with a different radial form—was used in refs 8 and 13. The Voronoi-CAP has, by definition, the same symmetry as the molecular system under consideration. However, it has sharp edges (Figure 1) at the boundaries between Voronoi cells, because it is continuous, but not continuously differentiable at the contact surfaces between the Voronoi cells. In principle, this effect should cause unnecessary reflections, yet it will turn out that these reflections are minimal, since not the CAP itself, but its representation in a Gaussian basis set matters. Nevertheless, the edges do lead to challenges in the numerical integration procedure (see below).

The second CAP is a smooth Voronoi-CAP, where the distance to the molecular system is defined through a weighted average (WA) of the distances to all nuclei:

$$r_{\text{WA}}(\vec{r}) = \sqrt{\frac{\sum_{\alpha} w_{\alpha} r_{\alpha}^2}{\sum_{\alpha} w_{\alpha}}} \quad (6)$$

where  $r_{\alpha}$  is the distance to nucleus  $\alpha$ , and the weights are computed according to

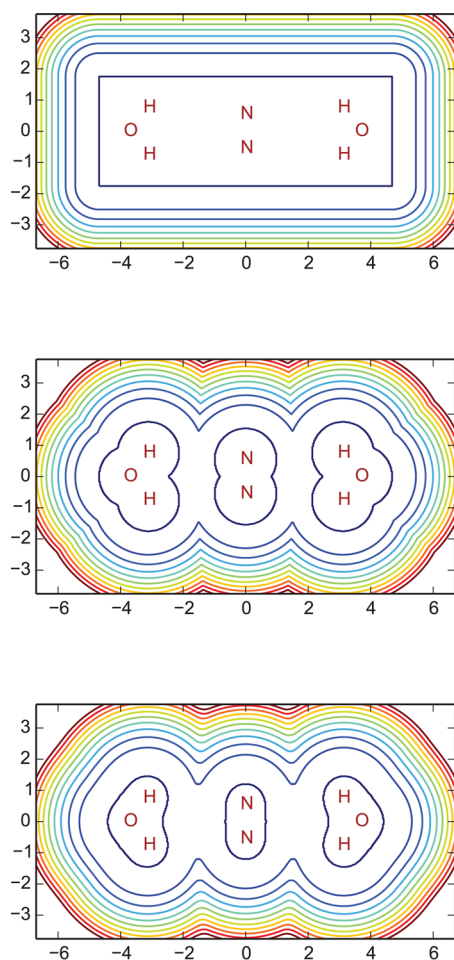


**Figure 1.** Contour plots of the three potentials used as CAPs. The respective potentials,  $W$  (c.f. eq 3), are shown using the model  $N_2(H_2O)_2$  cluster with  $r_{\text{cut}} = 1$  Å as an example. The top graph shows the box potential,  $W^{(B)}$  (eq 1), the graph in the middle shows the Voronoi potential,  $W^{(V)}$  (eq 5), and the bottom graph shows the smooth Voronoi potential,  $W^{(SV)}$  (eq 8). Contour lines are drawn starting at 0 in the center and increase in steps of 2 hartree up to 20 hartree.

$$w_\alpha = \frac{1}{(r_\alpha^2 - r_{\text{nearest}}^2 + 1 \text{ a.u.})^2} \quad (7)$$

Weights are large for atoms, which have distances that are similar to the nearest one, and vice versa, so that essentially only the distances to the few nearest atoms have appreciable weights. The smooth Voronoi-CAP is then defined in complete analogy to the Voronoi-CAP:

$$W^{(SV)}(\vec{r}) = W^{(SV)}(r_{\text{WA}}) = \begin{cases} 0 & r_{\text{WA}} \leq r_{\text{cut}} \\ (r_{\text{WA}} - r_{\text{cut}})^2 & r_{\text{WA}} > r_{\text{cut}} \end{cases} \quad (8)$$

The resulting CAP is much smoother than the Voronoi-CAP (Figure 1) and therefore more amenable to numerical integration.

The integrand of the integral that must be evaluated numerically is then a product of a Gaussian, which is a product of two primitive Gaussian basis functions itself, and the potential  $W$ . Because of the definition of  $W$ , the integrand vanishes inside the valence region, and grid points are, by construction, only needed outside the space where the electron

density of the neutral molecule is appreciable. Therefore, standard grids similar to those typically used in density functional calculations seem unsuitable for CAP integrals; here, an alternative brute force approach was used, placing, for every integral, a single large grid (angular Lebedev grid<sup>16</sup> with 3470 points, and a radial grid of 500 equidistant points and Euler–Maclaurin quadrature) on the center of the respective product Gaussian function. The relative accuracy of this numerical procedure, as measured by application to the known integrals of the box-CAP potential, is  $\sim 10^{-9}$ , and it is limited by the angular quadrature. Careful tests with smaller grids have been performed and trajectories of resonance states have been found—despite some deviations in certain matrix elements involving molecular orbitals with highly oscillatory behavior—to be largely independent of grid quality, unless fairly small grids are used. Temporary anion resonances are associated with low-energy electrons and, therefore, molecular orbitals with relatively few nodes, and the CAP matrix elements of these orbitals are clearly converged, with respect to the grid.

**2.2. *Ab Initio* Methods.** The basis sets used in the *ab initio* calculations consist of Dunning’s correlation-consistent valence triple- $\zeta$  (cc-pVTZ)<sup>17</sup> set augmented with a different number of diffuse functions. For most calculations, the cc-pVTZ set was augmented with a (2s5p2d) set of diffuse functions, where even-scaled exponents starting from the smallest exponents for the respective angular momentum in the original basis set were used: an even scaling factor of 2 for s and d functions and an even scaling factor of 1.5 for p functions. The only exception is the basis set placed on the water molecules in the computations for the model  $N_2(H_2O)$  cluster. The basis set for H was not augmented, and the basis set for O was augmented with a (1s1p1d) set of even scaled diffuse functions (even scaling factor of 3 was used for all angular momenta). In all calculations, the experimental geometry was used for all monomers ( $N_2$ ,  $CH_2O$ ,  $CO_2$ , and  $H_2O$ ). The only distance changed is the  $N_2$ –oxygen distance of the model cluster, which is described in the text and indicated in Figure 5.

All electron attachment energies and SAC–CI vectors needed for the projected CAP calculations<sup>6,18</sup> were computed with the symmetry-adapted cluster-configuration interaction (SAC–CI) method<sup>19,20</sup> for electron attachment states with single and double substitutions in the cluster operators. The SAC–CI method is a so-called *direct* method: First, the correlated electronic ground state of the neutral molecule is computed, and then several attachment states ( $(N + 1)$  electron states) are computed *directly*, in other words, self-consistent-field wave functions for open-shell anions are avoided and the method naturally yields more than one state. The SAC–CI method is effectively equivalent to equation-of-motion coupled-cluster methods for electron attachment,<sup>21–23</sup> however, specific implementations differ in certain details such as approximations regarding the number of terms used for the cluster and electron attachment operators, and, in particular, the efficiency of the SAC–CI code used here is increased by pruning the number of operators through a second-order perturbation energy cutoff criterion.<sup>24</sup> Moreover, a direct algorithm was adopted where sigma-vectors are directly calculated including all the product (nonlinear) terms.<sup>25</sup> The SAC–CI calculations were done with the Gaussian 09 suite of programs, Revision B.01.<sup>26</sup>

### 3. RESULTS

In this section, first, the three CAPs described above—the Voronoi-CAP, the smooth Voronoi-CAP, and the box-CAP—



are compared with each other, using the  $^2\Pi_g$  resonance of  $N_2$ , the  $^2B_1$  resonance of  $CH_2O$ , and the  $^2\Pi_u$  resonance of  $CO_2$  as examples. Then, as a pilot application of the smooth Voronoi-CAP, a model  $N_2(H_2O)$  cluster that demonstrates the splitting of the  $^2\Pi_g$  resonance of  $N_2$  into two  $^2B_g$  components is investigated.

Figure 2 shows computed resonance energies and widths of the  $^2\Pi_g$  resonance of  $N_2$  obtained with the three different

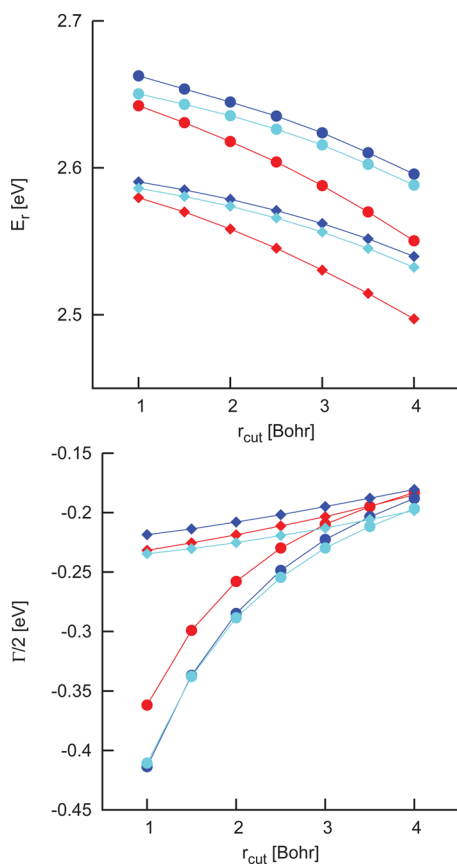


**Figure 2.** Results for the  $^2\Pi_g$  resonance of  $N_2$ . Compared are six sets of results, uncorrected (circles, ●) and corrected (diamonds, ◆) resonance energies for three different CAPs: box-CAP (red), Voronoi-CAP (blue), and smooth Voronoi-CAP (turquoise). The graph in the upper panel shows the real part of the resonance energy, and the graph in the lower panel shows the imaginary part of the resonance energy.

CAPs. The results for all three CAPs are consistent with the many results that have been computed for this “guinea-pig” state over time (see refs 9 and 27 for recent extensive collections of data) and—as one should expect—in excellent agreement with equation-of-motion coupled-cluster results obtained with the same valence basis.<sup>9,28,29</sup> Regarding comparison of the three different CAPs considered here, clearly, all three CAPs predict very similar results; yet, the box-CAP behaves slightly differently from the two Voronoi-CAPs. It predicts somewhat lower resonance energies, which are dependent somewhat more strongly on the cutoff parameter ( $r_{\text{cut}}$ ). However, the overall dependence on the cutoff parameter is very mild indeed: the uncorrected energies only change by  $\sim 0.05$  eV, while  $r_{\text{cut}}$  increases from 1 Bohr to 4 Bohr, and especially for the two Voronoi-CAPs, the corrected energies show an even smaller dependency.

Which value of  $r_{\text{cut}}$  is optimal is less clear-cut, since there is no apparent criterion to search for it. The speed of the trajectory at its most stable point seems to be an “obvious” choice; however, this is not so, as experience shows that a “pronounced” slowing is more indicative of a resonance than a low speed *per se*. Moreover, a pronounced stabilization is critical for identifying resonance states in cases where the assignment is not already known from prior information. The lowest speeds given in the Supporting Information should therefore be read with a grain of salt. Regarding these speeds, two comments are in order. First, the results seem to suggest that smaller  $r_{\text{cut}}$  values are better; yet, the price for that is a less “pronounced” stabilization up to the point where the uncorrected trajectories will not show any stabilization at all. Second, as shown in Figure 2, and the same is true for the other examples discussed below, the dependence of the computed resonance parameters on  $r_{\text{cut}}$  is normally weak and, in any case, much weaker than the dependence on the shape of the CAP, the one-particle basis set, and the electronic structure method. Thus, a detailed convergence study of  $r_{\text{cut}}$  seems only warranted once the other dependencies have been converged to the same level.

The imaginary part of the resonance energy is displayed in the second half of Figure 2 and shows a distinctly different trend. Similar to the real part, both the uncorrected and corrected values for the widths are dependent only weakly on which of the three CAPs is used. On the other hand, while the corrected widths show the same weak dependency on the cutoff parameter as the real resonance energy, the uncorrected widths are strongly dependent on the cutoff parameter for small  $r_{\text{cut}}$  before essentially converging to the corrected value for larger values of  $r_{\text{cut}}$  (Figure 2). Nevertheless, the main issue considered here is the dependency on the shape of the CAP, and for a molecule such as  $N_2$ , which easily fits into a box, there is clearly no significant difference between the box-CAP and Voronoi-CAP results.

With very slight variations, the trends established for the  $^2\Pi_g$  resonance of  $N_2$  can also be observed for the  $^2B_1$  resonance of  $CH_2O$  (Figure 3) and the  $^2\Pi_u$  resonance of  $CO_2$  (Figure 4). For both resonances, the results are in excellent agreement with earlier fixed-nuclei calculations, in particular, coupled cluster and SAC-CI calculations with similar valence basis sets.<sup>6,9,10,30</sup> For carbon dioxide, the uncorrected trajectories do not show any clear slowing and accelerating-again behavior, so only the corrected values can be reported, but apart from that the mild dependency of both, corrected and uncorrected, resonance energy as well as corrected widths on the cutoff parameter can clearly be observed in the figures. The correction itself is small, with the exception of the resonance width at small cutoff parameters. So, coming back to the main point, the dependence of the resonance parameters on the shape of the CAP is, again, essentially negligible. Clearly, all these small symmetric molecules fit well into a box, and our results show that Voronoi-CAPs and the box-CAP work equally well in this type of situation.

As a first pilot application of the new CAP, a model  $N_2(H_2O)$  cluster with  $D_{2h}$  symmetry (Figure 5) is considered. We use the smooth Voronoi-CAP rather than the Voronoi-CAP (c.f. Figure 1) in these calculations, because of its better performance in the numerical integrations (see section 2). The two water molecules provide an environment for the nitrogen molecule, and when the water molecules are brought in from infinity to a finite distance  $R$ , the two components of the  $^2\Pi_g$

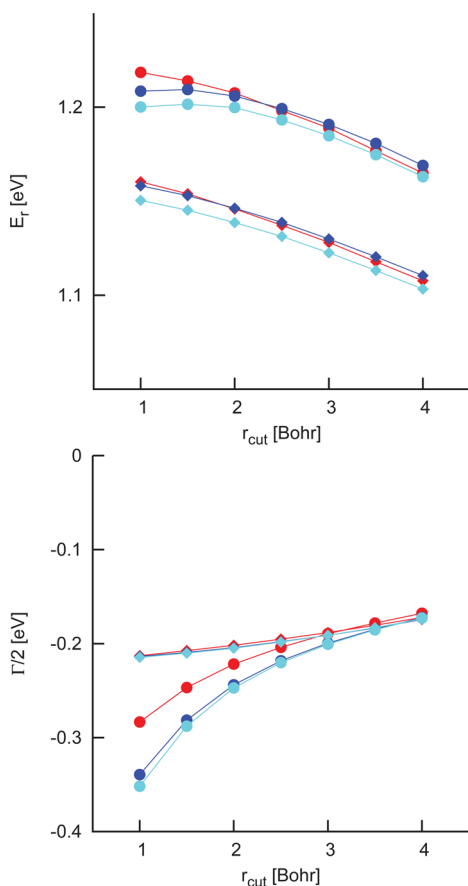


**Figure 3.** Results for the  $^2B_1$  resonance of  $\text{CH}_2\text{O}$ . Compared are six sets of results, uncorrected (circles, ●) and corrected (diamonds, ◆) resonance energies for three different CAPs: box-CAP (red), Voronoi-CAP (blue), and smooth Voronoi-CAP (turquoise). The graph in the upper panel shows the real part of the resonance energy, and the graph in the lower panel shows the imaginary part of the resonance energy.

resonance state of  $\text{N}_2^-$  will be split into two  $^2B_g$  components. The energy of the neutral model cluster shows a shallow minimum at  $R \approx 3.7$  Å, and the repulsive potential becomes noticeable for distances below 3.2 Å or so (see Figure 6).

Resonance energies and widths of the two  $^2B_g$  resonance states have been studied as a function of  $R$ , and the results are shown in Figure 6. In the standard orientation of the Gaussian program, the cluster is put in the  $xy$ -plane with the  $\text{N}_2$  molecule in the  $y$ -axis so that the out-of-plane  $^2\Pi_u$  component becomes a  $^2B_{1g}$  state and the in-plane component becomes a  $^2B_{3g}$  state. Because of the orientation of the water dipoles, both components are stabilized by the environment, and this trend is reflected in the changes of their resonance energies and widths (note that, in Figure 6, the resonance energy is the difference between the potential energy curve of the neutral and that of the respective anion and the width is indicated as an “error bar”). Yet, as one would expect, the in-plane component interacts with the water molecules far more strongly: At  $R = 2.4$  Å (the leftmost point in Figure 6), the resonance energy of this component has been reduced from 2.57 eV for unperturbed  $\text{N}_2^-$  to 0.45 eV, and its half width has decreased by 2 orders of magnitude, from 0.22 eV to 0.0025 eV.

Coming back to our main point, the difference between the Voronoi-CAPs and the box-CAP, the same calculation has been repeated with the box-CAP and the widths, which are the more sensitive indicators, are compared in Figure 7. As expected, the

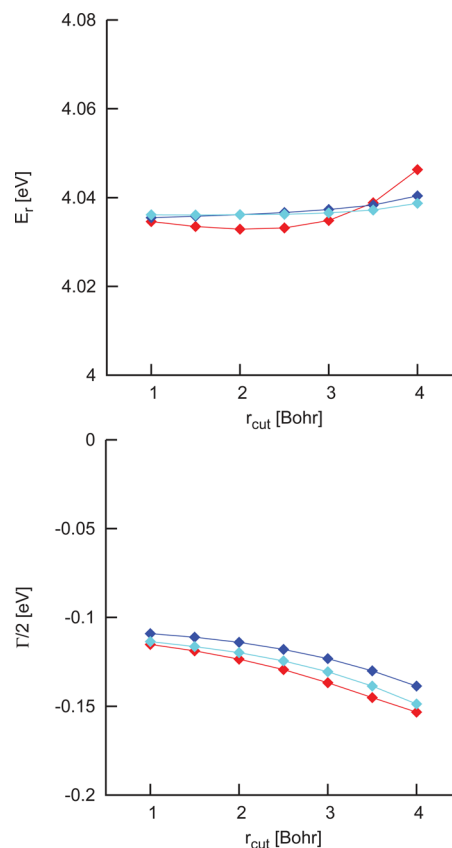


**Figure 4.** Results for the  $^2\Pi_u$  resonance of  $\text{CO}_2$ . Compared are corrected resonance energies for three different CAPs: box-CAP (red), Voronoi-CAP (blue), and smooth Voronoi-CAP (turquoise). The graph in the upper panel shows the real part of the resonance energy, and the graph in the lower panel shows the imaginary part of the resonance energy.

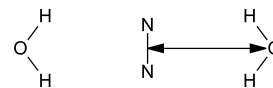


**Figure 5.** Geometry of the  $\text{N}_2(\text{H}_2\text{O})$  model cluster. Resonance states of  $\text{N}_2$  are investigated as a function of the distance of the oxygen atoms from the N–N axis indicated as in the figure while keeping the cluster  $D_{2h}$  symmetric.

results are dependent only weakly on the CAP shape and run almost perfectly parallel for the out-of-plane  $^2B_{1g}$  state—similar to the three small molecules studied above. However, this is not so for the in-plane  $^2B_{3g}$  state: For small  $\text{H}_2\text{O}$ – $\text{N}_2$  distances, the two  $\Gamma$  curves in Figure 7 are almost on top of each other, but for larger distances, they deviate considerably (by more than 0.2 eV), with the box-CAP yielding the much larger  $\Gamma$  values. This demonstrates clearly the effect of the “dead space” between the  $\text{N}_2$  and the  $\text{H}_2\text{O}$  molecules, where, if a box-CAP is used, there is neither an absorbing region nor a satisfactory description with the atom centered basis functions so that artifacts from reflections, which result in widths that are too high, arise.

## 4. CONCLUSIONS

The three basic ingredients of a CAP calculation are the electronic structure method employed to compute the eigenstates of the CAP Hamiltonian, the underlying one-particle basis set, and the CAP itself. In the past, the box-CAP (eq 1) has been the workhorse of most CAP applications in

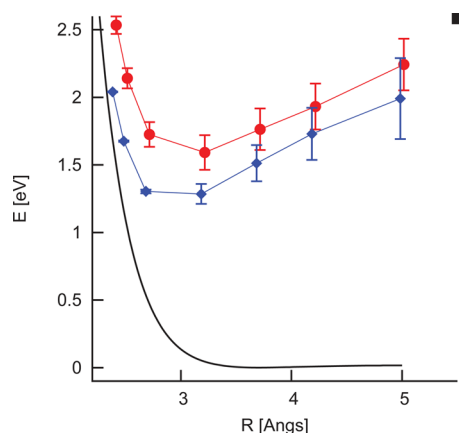


**Figure 6.** Potential energy curve of the  $\text{N}_2(\text{H}_2\text{O})$  model cluster. The coordinate  $R$  on the abscissa is the distance of the oxygen atoms from the  $\text{N}-\text{N}$  axis (c.f. Figure 5). The energy of the neutral  $N$  electron ground state is shown as a black line, and electron attachment leads to two  $(N + 1)$  electron  ${}^2\text{B}_g$  states, which correspond asymptotically to the  ${}^2\Pi_g$  resonance of  $\text{N}_2$ : a  ${}^2\text{B}_{1g}$  state (red circles, ●) and a  ${}^2\text{B}_{3g}$  state (blue diamonds, ◆). The “error bars” in the plot indicate the full width of the resonance states. As a reference, the asymptotic value of the  $\text{N}_2$   ${}^2\Pi_g$  resonance energy computed with the same method/basis set combination is indicated as a black square.

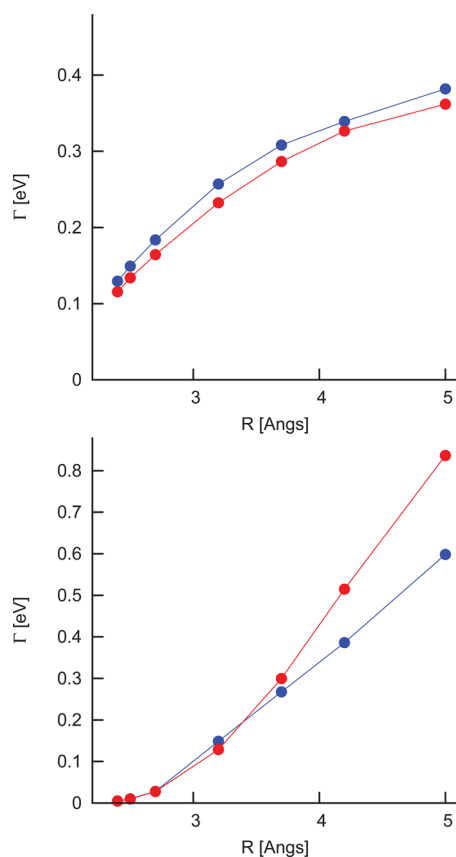


**Figure 7.** Widths of the out-of-plane  ${}^2\text{B}_{1g}$  (upper panel) and in-plane  ${}^2\text{B}_{3g}$  (lower panel)  $\text{N}_2^-$  resonance states of the embedded  $\text{N}_2(\text{H}_2\text{O})_2$  model cluster computed with the smooth Voronoi-CAP (blue) and the box-CAP (red).

electronic structure theory contexts, because of the ease of the evaluation of its integrals in a Gaussian basis set. Here, two new CAPs have been systematically investigated: the Voronoi-CAP

(eq 5) and the smooth Voronoi-CAP (eq 8). The disadvantage of the two new CAPs is the need to perform numerical integrations; the great advantage is that they wrap perfectly around the molecular systems considered. Not only does this CAP choice guarantee that the CAP and the molecular system have the same symmetry, but more importantly that the CAP wraps around any side chain or any monomer of a cluster, independent of how far away a monomer may be from the rest of the cluster.

As a first check, the performance of the new CAPs was compared with that of the box-CAP for the well-understood resonances of  $\text{N}_2$ ,  $\text{CH}_2\text{O}$ , and  $\text{CO}_2$ . Note that, for a meaningful comparison, the same electronic structure method and basis sets must be used throughout (here, SAC-Cl, cc-pVTZ augmented with a  $(2s5p2d)$  set); however, our results for all classical test cases agree well with other fixed-nuclei results in the literature (of course, in particular, with equation-of-motion coupled-cluster results obtained with triple- $\zeta$  valence basis sets, since those are very similar method/basis set combinations). Since all three test cases are small symmetric molecules, no large differences between the results for the three CAPs are expected, and that is indeed what is found. Depending on the cutoff parameter ( $r_{\text{cut}}$ ), the differences can grow up to 0.05 eV, but typical differences are in the order of 0.01 eV, in particular for the corrected results.

In addition to showing that the Voronoi-CAPs and the box-CAP are equally valid choices for symmetric systems, our  $\text{N}_2$ ,  $\text{CH}_2\text{O}$ , and  $\text{CO}_2$  results represent a systematic investigation of the dependence on  $r_{\text{cut}}$ , which, because of the different CAP definitions, is defined somewhat differently itself for each CAP (c.f. eqs 1, 5, and 8). While  $r_{\text{cut}}$  changes over the wide range of 1–4 Bohr, both the uncorrected and corrected computed resonance positions typically change by only a few hundredths of an electron volt and the same is true for the corrected half widths. Hence, not only is the dependence of the computed parameters on the cutoff radius small, it is also much weaker than the dependence on the electronic structure method, the one-particle basis set, and the general functional form of the CAP itself.

Last, as a first pilot application, the model cluster  $\text{N}_2(\text{H}_2\text{O})_2$  ( $D_{2h}$  symmetrical conformation) was investigated. The model demonstrates how the  ${}^2\Pi_g$  resonance of  $\text{N}_2$  is split in a stabilizing environment into two  ${}^2\text{B}_g$  components, and the lower of the two is clearly on the way to be turned into a stable state, although at distances where the neutral cores already show a substantial repulsion. In these calculations, the smooth Voronoi-CAP was exclusively used (because of its smoother functional form, it is more amiable to numerical integration than the Voronoi-CAP). Since the model cluster is highly symmetric and essentially two-dimensional, one might be tempted to think that the box-CAP would work equally well for this specific example; however, this is only true for small  $\text{N}_2-\text{H}_2\text{O}$  distances. At larger distances, the results for the in-plane component clearly show effects from artifacts stemming from the “dead space” between the molecules of a cluster (c.f. Figure 1) where, if a box-CAP is used, there is neither a CAP nor a satisfactory description with atom-centered Gaussians.

Thus, a Voronoi-type CAP is not only far easier to use but also the superior choice, as it does not leave any “dead space” between the molecules of a cluster (c.f. Figure 1) or any parts of a single larger molecule, which does not fit easily into a box. Dead space in itself would not be problematic—provided it was filled with a flexible basis set. Unfortunately, this is hard to

guarantee with atom-centered Gaussians, and the larger the space that is far from atoms and not filled by a CAP, the more sources of artificial reflections are introduced into a CAP calculation. One example where one may rather choose to fill dead space—possibly with ghost centers—are interacting resonances on two different molecules. On the other hand, it is easy to take our model and go further and construct three-dimensional model environments such as a Kevan solvation shell, where the box-CAP will completely break down for large radii of the solvation shell, while a Voronoi-CAP will continue to work normally.

## ■ ASSOCIATED CONTENT

### ● Supporting Information

This material is available free of charge via the Internet at <http://pubs.acs.org/>. The Supporting Information is available free of charge on the ACS Publications website at DOI: 10.1021/acs.jctc.5b00465.

Figures shown in the Supporting Information complement Figures 2, 3, and 4 of the main text. They show the logarithmic speed of the corrected and uncorrected trajectories,  $\ln dE(\eta)/d\eta$  and  $\ln^2 dE(\eta)/d^2\eta$  (c.f. eqs 139 and 140 of ref 1), which are used to determine the “stability” of the trajectories. The optimal value of  $\eta$  is dependent on  $r_{\text{cut}}$  but is—at least for these small symmetric molecules—fairly independent of the CAP, and falls into the range of  $5 \times 10^{-4}$ – $5 \times 10^{-2}$  with smaller  $r_{\text{cut}}$  values being clearly associated with smaller optimal  $\eta$  (PDF)

## ■ AUTHOR INFORMATION

### Corresponding Authors

\*E-mail: [Thomas.Sommerfeld@selu.edu](mailto:Thomas.Sommerfeld@selu.edu) (T. Sommerfeld).

\*E-mail: [ehara@ims.ac.jp](mailto:ehara@ims.ac.jp) (M. Ehara).

### Notes

The authors declare no competing financial interest.

## ■ ACKNOWLEDGMENTS

Acknowledgment is made to the donors of the American Chemical Society Petroleum Research Fund for support of this research.

## ■ REFERENCES

- (1) Santra, R.; Cederbaum, L. S. *Phys. Rep.* **2002**, *368*, 1–117.
- (2) Sajeev, Y.; Ghosh, A.; Vaval, N.; Pal, S. *Int. Rev. Phys. Chem.* **2014**, *33*, 397–425.
- (3) Sommerfeld, T.; Riss, U. V.; Meyer, H.-D.; Cederbaum, L. S.; Engels, B.; Suter, H. U. *J. Phys. B: At., Mol. Opt. Phys.* **1998**, *31*, 4107.
- (4) Sommerfeld, T.; Tarantelli, F.; Meyer, H.-D.; Cederbaum, L. S. *J. Chem. Phys.* **2000**, *112*, 6635.
- (5) Feuerbacher, S.; Sommerfeld, T.; Santra, R.; Cederbaum, L. S. *J. Chem. Phys.* **2003**, *118*, 6188.
- (6) Ehara, M.; Sommerfeld, T. *Chem. Phys. Lett.* **2012**, *537*, 107.
- (7) Ghosh, A.; Vaval, N.; Pal, S. *J. Chem. Phys.* **2012**, *136*, 234110.
- (8) Krause, P.; Sonk, J. A.; Schlegel, H. B. *J. Chem. Phys.* **2014**, *140*, 174113.
- (9) Zuev, D.; Jagau, T.-C.; Bravaya, K. B.; Epifanovsky, E.; Shao, Y.; Sundstrom, E.; Head-Gordon, M.; Krylov, A. I. *J. Chem. Phys.* **2014**, *141*, 024102.
- (10) Ghosh, A.; Vaval, N. *J. Chem. Phys.* **2014**, *141*, 234108.
- (11) Riss, U. V.; Meyer, H.-D. *J. Phys. B: At., Mol. Opt. Phys.* **1993**, *26*, 4503.
- (12) Santra, R.; Cederbaum, L. S.; Meyer, H.-D. *Chem. Phys. Lett.* **1999**, *303*, 413.
- (13) Krause, P.; Schlegel, H. B. *J. Chem. Phys.* **2014**, *141*, 174104.
- (14) Riss, U. V.; Meyer, H.-D. *J. Chem. Phys.* **1996**, *105*, 1409.
- (15) Riss, U. V.; Meyer, H.-D. *J. Phys. B: At., Mol. Opt. Phys.* **1998**, *31*, 2279.
- (16) Lebedev, V. I.; Laikov, D. N. *Dokl. Math.* **1999**, *59*, 477.
- (17) Dunning, T. H., Jr. *J. Chem. Phys.* **1989**, *90*, 1007.
- (18) Sommerfeld, T.; Santra, R. *Int. J. Quantum Chem.* **2001**, *82*, 218.
- (19) Nakatsuji, H. *Chem. Phys. Lett.* **1979**, *67*, 329.
- (20) Nakatsuji, H. *Chem. Phys. Lett.* **1979**, *67*, 334.
- (21) Nooijen, M.; Bartlett, R. J. *J. Chem. Phys.* **1995**, *102*, 3629.
- (22) Stanton, J. F.; Bartlett, R. J. *J. Chem. Phys.* **1993**, *98*, 7029–7039.
- (23) Mertins, F.; Schirmer, J.; Tarantelli, A. *Phys. Rev. A: At., Mol., Opt. Phys.* **1996**, *53*, 2153.
- (24) Nakatsuji, H. *Chem. Phys.* **1983**, *75*, 425.
- (25) Fukuda, R.; Nakatsuji, H. *J. Chem. Phys.* **2008**, *128*, 094105.
- (26) Frisch, M. J.; Trucks, G. W.; Schlegel, H. B.; Scuseria, G. E.; Robb, M. A.; Cheeseman, J. R.; Scalmani, G.; Barone, V.; Mennucci, B.; Petersson, G. A.; Nakatsuji, H.; Caricato, M.; Li, X.; Hratchian, H. P.; Izmaylov, A. F.; Bloino, J.; Zheng, G.; Sonnenberg, J. L.; Hada, M.; Ehara, M.; Toyota, K.; Fukuda, R.; Hasegawa, J.; Ishida, M.; Nakajima, T.; Honda, Y.; Kitao, O.; Nakai, H.; Vreven, T.; Montgomery, J. A. Jr.; Peralta, J. E.; Ogliaro, F.; Bearpark, M.; Heyd, J. J.; Brothers, E.; Kudin, K. N.; Staroverov, V. N.; Kobayashi, R.; Normand, J.; Raghavachari, K.; Rendell, A.; Burant, J. C.; Iyengar, S. S.; Tomasi, J.; Cossi, M.; Rega, N.; Millam, J. M.; Klene, M.; Knox, J. E.; Cross, J. B.; Bakken, V.; Adamo, C.; Jaramillo, J.; Gomperts, R.; Stratmann, R. E.; Yazyev, O.; Austin, A. J.; Cammi, R.; Pomelli, C.; Ochterski, J. W.; Martin, R. L.; Morokuma, K.; Zakrzewski, V. G.; Voth, G. A.; Salvador, P.; Dannenberg, J. J.; Dapprich, S.; Daniels, A. D.; Farkas, A.; Foresman, J. B.; Ortiz, J. V.; Cioslowski, J.; Fox, D. J. *Gaussian 09 Revision B.01*; Gaussian, Inc.: Wallingford, CT, 2009.
- (27) Horáček, J.; Mach, P.; Urban, J. *Phys. Rev. A: At., Mol., Opt. Phys.* **2010**, *82*, 032713.
- (28) Ghosh, A.; Karne, A.; Pal, S.; Vaval, N. *Phys. Chem. Chem. Phys.* **2013**, *15*, 17915.
- (29) Jagau, T.-C.; Zuev, D.; Bravaya, K. B.; Epifanovsky, E.; Krylov, A. I. *J. Phys. Chem. Lett.* **2014**, *5*, 310.
- (30) Sommerfeld, T.; Ehara, M. *J. Chem. Phys.* **2015**, *142*, 034105.